Author Manuscript

Author Manuscript

Author Manuscript

Author Manuscript

HHS Public Access

Author manuscript

J Mol Biol. Author manuscript; available in PMC 2015 August 13.

Published in final edited form as:

J Mol Biol. 2011 December 16; 414(5): 723–734. doi:10.1016/j.jmb.2011.10.030.

Crystal structure of the ligand-binding domain of Netrin-G2

Julia Brasch[1], **Oliver J. Harrison**[1,2], **Goran Ahlsen**[1], **Qun Liu**[3], and **Lawrence Shapiro**[1]

[1]Department of Biochemistry and Molecular Biophysics, Columbia University, 701 West 168th Street, New York, NY 10032, USA

[2]Howard Hughes Medical Institute, Columbia University, 1130 St. Nicholas Avenue, New York, NY 10032, USA

[3]New York Structural Biology Center, NSLS X4, Brookhaven National Laboratory, Upton, NY 11973, USA

Abstract

Netrin G proteins represent a small family of synaptic cell adhesion molecules related to netrins and to the polymerization domains of laminins. Two netrin G proteins are encoded in vertebrate genomes, netrins G1and G2, which are known to bind the leucine-rich repeat proteins netrin G ligands (NGLs) 1 and 2, respectively. Netrin G proteins share a common multi-domain architecture comprising an laminin N-terminal (LN) domain followed by three Laminin-EGF (LE) domains and a C′ region containing a GPI anchor. Here we use deletion analysis to show that the LN domain region of netrin Gs contains the binding site for NGLs to which they bind with 1:1 stoichiometry and sub-micromolar affinity. Netrin Gs are alternatively spliced in their LE domain regions, but the binding region, the LN domain, is identical in all splice forms. We determined the crystal structure for a fragment comprising the LN domain and domain LE1 of Netrin G2 by Sulfur-SAD phasing and refined it to 1.8Å resolution. The structure reveals an overall architecture similar to laminin α chain LN domains, but includes significant differences including a Ca^{2+} binding site in the LN domain. These results reveal the minimal binding unit for interaction of netrin Gs with NGLs, define structural features specific to netrin Gs, and suggest that netrin G alternative splicing is not involved in NGL recognition.

Keywords

NGL; Netrin; Laminin; Cell-adhesion molecules; Sulfur-SAD

INTRODUCTION

Netrin Gs are a small family of synaptic cell adhesion proteins in vertebrates that are related by sequence to classical netrins and laminins. They are predominantly expressed in the brain and central nervous system[1; 2] where they promote neurite outgrowth[1; 3], regulate excitatory

Correspondence should be addressed to L.S. (LSS8@columbia.edu); Department of Biochemistry and Molecular Biophysics, Columbia University, 635 West 165th Street, New York, NY 10033, USA; phone: 1-212-342-6029; fax: 1-212-342-6026.

Accession number. Coordinates and structure factors for the described crystal structure of human Netrin G2 comprising domains LN and LE1 have been deposited in the PDB under accession number: **3TBD**

Author Manuscript Author Manuscript Author Manuscript Author Manuscript

synapse formation[4] and mediate lamina specific sub-dendritic compartmentalization[5]. Two different subtypes of netrin Gs have been identified: netrin G1[2; 6] and netrin G2[1; 6], for which discrete and complimentary expression patterns marking distinct brain regions have been observed[1; 5]. Netrin Gs interact trans-neuronally with their binding partners, netrin G ligands (NGLs) 1 and 2, members of a small group of leucine-rich repeat containing cell adhesion proteins[4; 5]. Binding is isoform specific, since netrin G1 and netrin G2 bind to NGL-1 and NGL-2, respectively[3; 4; 5; 7; 8]. Netrin Gs are localized preferentially on projecting, presynaptic axons[5], whereas NGLs localize postsynaptically on dendrites[4; 5]. Gene ablation studies show that NGL-1 and NGL-2 are mis-localized in mice that lack either netrin G1 or netrin G2, respectively[5] and loss of either netrin-G2 or NGL-2 results in impairment of the responsiveness of auditory neurons [8].

The overall domain organization of netrin Gs is highly similar to that of classical netrins, which are secreted axon guidance molecules[9], and to the polymerization region of laminins[10] (Fig. 1). Netrin Gs are extracellular proteins composed of a large N-terminal domain of 268 amino acids in length, referred to as the laminin N-terminal (LN)-domain of netrin G (previously also referred to as domain VI), followed by three consecutive cysteine rich laminin EGF-like (LE) domains each of approximately 55 amino acids, and a C-terminal C′ domain of approximately 60 amino acids, which is suggested to contain a non laminin-like EGF motif[6]. Despite their similar overall domain organization, netrin Gs differ from classical netrins in several respects. Domain C of classical netrins contains basic amino acids, which bind to plasma membrane and extracellular matrix structures such as heparin, heparan sulfate proteoglycans and membrane glycolipids[9]. In contrast, netrin Gs have a hydrophobic region in their C′ domain to which a glycosyl-phosphatidyl-inositol (GPI) anchor is attached, anchoring the netrin Gs to the plasma membrane[1; 2; 6]. Netrin Gs also differ from classical netrins in that they are found exclusively in vertebrates[1; 2; 6], whereas classical netrins also have homologues in invertebrates and, additionally, netrin Gs fail to bind to the classical netrin receptors DCC and Unc5h[1; 2; 6]. Netrin G1 and netrin G2 each have multiple splice forms, 14 for netrin G1 (netrin G1a-o) and three for netrin G2 (netrin G2a-c), which differ by amino acid insertions of different lengths after domain LE1 or by deletion of different combinations of LE-domains[1; 6; 11]. For netrin G2, splice isoforms may contain an insertion of 59 (netrin G2b) or 34 amino acids (netrin G2c) between domains LE1 and LE2 (Fig. 1)[1;6]. Expression of splice isoforms appears to be spatiotemporally regulated in the brain and, although very limited, expression outside the nervous system for some splice isoforms was found[11].

NGLs, the binding partners of netrin Gs, are single-pass transmembrane proteins with an extracellular domain (approximately 308 amino acids) comprised of a nine leucine rich repeat (LRR) region capped by N- and C-terminal cysteine rich domains, followed by a C2-type immunoglobin (Ig) domain of about 107 residues, a transmembrane domain and a cytoplasmic domain of approximately 100 amino acids including a PDZ-binding motif at the C-terminus, which mediates binding to PSD-95[3; 4; 12; 13]. Domain-deletion studies, in which N- and C-terminally truncated fragments of NGL-1 were tested for binding to netrin G1 in solid phase binding assays, showed the LRR domain of NGL-1 to be necessary and sufficient for heterophilic interaction with netrin G1, with the Ig domain playing no direct role[3].

Author Manuscript Author Manuscript Author Manuscript Author Manuscript

The binding mode and mechanism of specificity for netrin G/NGL interaction, including the role of alternative splicing, remain unknown. The minimal NGL-binding domain of netrin G has not yet been identified, and atomic-level structures do not yet exist for any classical netrin or netrin G family member. We therefore set out to identify the NGL-binding domain of netrin Gs using domain deletion studies, and to determine the atomic resolution structure of a fragment of netrin G2 containing the NGL binding region. Our results localize the NGL binding domain of netrin Gs to the LN domain, identify structural features unique to this small family of synaptic cell adhesion and signaling molecules, and suggest that alternative splicing of netrin G1 and G2 has no influence on the heterophilic binding to their NGL binding partners.

RESULTS

The LN domain of Netrin G contains the NGL binding region

To investigate the binding between netrin G and netrin G ligand in solution and to determine the minimal region of netrin G responsible for ligand binding, we expressed and purified extracellular fragments of human netrin G1, netrin G2 and the whole extracellular regions from their respective binding partners netrin G ligand (NGL) 1 and 2 (Fig. 1). Previous studies demonstrate that the netrin G binding site in the NGL ectodomain is localized to the LRR region[3], however, no similar analysis has been reported for the netrin G side of the interaction.

We first characterized the binding of full-length netrin G2 lacking only the GPI anchor site to a full length NGL-2 extracellular fragment by sedimentation equilibrium analytical ultracentrifugation (AUC). On their own, both netrin G2 and NGL-2 ectodomains were found to be monomeric in solution with apparent molecular weights from AUC corresponding closely to monomer molecular weights determined by mass spectrometry (Table 1). When an equimolar mixture of these fragments was analyzed, a monomer/dimer equilibrium was observed in AUC with an apparent molecular weight of 100kDa indicating high affinity heterodimerization with a stoichiometry of 1:1 (Table 1). Fitting of the data to a 1:1 binding model yielded a K_D value for heterodimerization of 0.2μM, in agreement with previous SPR studies[5]. Binding between netrin G2 and NGL-2 was found to be calcium independent, since similar results were observed in the presence of either 3mM $CaCl_2$ or 1mM EDTA in the buffers (Table 1), as observed previously in cell binding experiments[4].

To identify the minimal ligand binding fragment of netrin Gs by domain, we tested additional netrin G fragments that were truncated at the C-terminus. One fragment of netrin G2 encompassing domains VI and LE1 only (sNetrin G2, see Fig. 1) showed binding to NGL-2 with a K_D value almost identical to that for binding between full length fragments (Table 1), suggesting that the ligand binding site resides within the two most N-terminal domains of netrin G2. We attempted to delineate the binding site further by preparing a netrin G2 fragment containing the LN domain only, however poor stability of this protein precluded further analysis. To overcome this, we analyzed instead the netrin G1 isoform for which several naturally occurring C-terminally truncated splice forms have been described in mouse[1; 6; 11]. We expressed two of these fragments: netrin G1f comprising the LN and LE1 domain and netrin G1j comprising the LN domain only (Fig. 1). Exactly as observed

Author Manuscript Author Manuscript Author Manuscript Author Manuscript

for the analogous sNetrin G2 fragment, netrin G1f bound to its ligand, NGL-1, with high affinity and 1:1 stoichiometry in AUC experiments (Table 1). Importantly, the netrin G1j fragment also bound to NGL-1 with comparable affinity (Table 1), showing that ligand binding of netrin G proteins is localized to the LN domain.

Structure of sNetrin G2

Based on the apparent localization of the netrin G NGL binding site to the LN domain, we sought to produce crystals of constructs containing this region. Diffracting crystals of the sNetrin G2 protein, which includes the LN and the adjacent LE1 domain, were produced with conditions containing 20 % (w/v) PEG 3,350, 200 mM Calcium acetate, 100 mM Sodium cacodylate, pH 6.5. These crystals belong to space group $P3_221$ with cell constants a=b=64.13 Å, c=190.64 Å, and diffract x-rays beyond 1.8 Å Bragg spacings (Table 2). The sNetrin G2 protein contains 16 cysteine residues. At the absorption edge of Fe Kα (λ=1.7432 Å), the calculated anomalous contribution to the total scattering <ΔF>/<F> is 1.34%, suggesting the possibility for phase determination by measuring the anomalous scattering of the endogenous sulfur atoms. A multi-crystal sulfur single wavelength anomalous diffraction (SAD) experiment was performed with five frozen crystals[14]. The multi-crystal sulfur-SAD data were measured at 2.3 Å and the resulting phases were extended to 1.8 Å with a high resolution native data set. The 1.8Å experimental electron density map is shown in Fig. 2a. The map is of extraordinary quality, with clear density for all regions with the exception of poorly ordered loops at Thr11-14 and His54-Tyr58. An initial model was auto-built using ARP/WARP[15] and the model was refined to an R-factor of 0.179 and R_{free} 0.212 using Coot[16] and Refmac[17].

The overall structure of sNetrin G2 is comprised of a large N-terminal domain, the LN domain, and smaller LE1 domain (Fig. 2b). The overall dimensions of the structure are ~70Å in the long axis (vertical in Fig. 1a) by 40Å by 25Å. The larger N-terminal domain has dimensions 40Å x 40Å x 25Å excluding the N-terminus which extends down to the level of LE1 as a disulfide-locked two-stranded β-sheet that interacts near its base with the C-terminal LE1 domain. The LN domain, similar to the recently determined structure of the related (30% identity) laminin α chain LN domain[18], adopts a jelly roll topology β-sandwich fold with numerous loop and helical excursions from the domain body. As pointed out previously [18; 19], the topology of this domain is similar to that of bacterial galactose binding domains. A Ca^{2+} binding site (Fig. 2c), absent in laminin α but present in galactose binding domains, is found between Leu77-Thr88. The bound Ca^{2+} ion contributed significantly to the anomalous scattering in the diffraction experiments at 1.8Å, and was used in phase calculations equivalently to sulfur.

The LN domain has many loop and helix excursions that elaborate the jelly roll core. The first of these, at the N-terminus, comprises two β-strands that form a two-stranded hairpin sheet that precedes the main body of the LN domain. This hairpin sheet has a disulfide bond between the two strands at cysteines 5 and 22. This disulfide itself, as well as nearby residues from the hairpin strands including Tyr2, Phe19, Ala21, and Pro24, which are all conserved in character across netrin Gs, but not other related domains, pack against the LE1 domain. These interactions, as well as interactions between LE1 and the base of the LN

Author Manuscript Author Manuscript Author Manuscript Author Manuscript

domain, particularly elements of β4 and the large helical excursion between β8 and β9, suggest a rigid connection between the LN and LE1 domain.

At the apex of the LN domain, a large excursion essentially devoid of secondary structure is comprised by residues Ser40 to Glu103, and includes two disulfide bonds: one between cysteines 44 and 64, which is conserved in all related domains (Fig. 3b), and the other between cysteines 52 and 60, which is conserved among netrin Gs. This large excursion region is well resolved in the sNetrin G2 structure, but most of the analogous region in laminin α is disordered and revealed no electron density that could be modeled[18].

The last two excursive regions, the first of which emanates from between β7 and β8, and the second between β8 and β9, pack together to form a helical sub-region. The β7-β8 excursion region includes two small helices and a single disulfide bond between cysteines 154 and 178. The protomer-facing side of this excursion packs against the β8- β9 excursion which comprises residues Glu197-Lys227. These two regions appear together to form a rigid structure, the base of which interacts with the apex of the LE1 domain through a hydrophobic mini-core centered around Tyr217 from the β8- β9 region and Tyr316 from the LE1 domain.

The LN domain includes a Ca^{2+} binding site, present in galactose binding domains, but absent in laminin $\alpha_{18;}$ [20]. Ligands to the Ca^{2+} ion are donated by seven ligands in the classical pentagonal bipyramid mode, with five planar ligands donated from the β3- β4 excursion including side chain oxygen atoms of Asp80, Glu82, and Thr88, and backbone carbonyls from Leu77 and Thr88 (Fig. 2c). Of the two axial ligands, one is donated from a water molecule, and the second from the backbone carbonyl of Ser262 on the β10 strand. This interaction appears to pin the β3- β4 excursion to the main body of the protomer. Residues with side chains that donate Ca^{2+}-binding ligands, Asp80, Glu82, and Thr88, are conserved in netrin Gs, but not in other related domains, eg classical netrins and laminin α LN domains (Fig. 3d) and also not in laminin β and γ chains, suggesting that Ca^{2+} binding is a conserved feature of netrin Gs. As described above, binding between netrin G and NGL is calcium independent, so the function of this calcium binding site remains to be determined.

All proteins described here were produced in mammalian cells, and hence are expected to be glycosylated. N-linked glycans are observed in the experimental and refined electron density maps for Asn105 and Asn111, both in the β4 strand (Fig. 2b). Asn105 is conserved in all netrin Gs, netrins, and laminins, however Asn111, while conserved in netrin G2s across species, is present in netrin G1 only in some species (Fig. 3).

The LE1 domain of sNetrin G2 exhibits a topology and disulfide bonding pattern identical to that previously characterized for the LE domains from laminins α and γ[18; 21]. Briefly, the LE1 domain is devoid of regular secondary structure, but is stabilized by a core of four disulfide bonds: Cys270-Cys279, Cys272-Cys288, Cys290-Cys299, and Cys302-Cys327 (Fig. 2b). As mentioned above, two loops from LE1 encompassing residues 279–288 and 313–325 extend from the disulfide-bonded core to interact with the base of the LN domain, apparently rigidifying the interdomain connection. This latter loop also interacts with the N-

Author Manuscript Author Manuscript Author Manuscript Author Manuscript

terminal β-hairpin that extends downward from the LN domain, potentially providing further rigidity.

Related domains from laminins and netrins

Netrin Gs show significant sequence similarity to classical netrins, and to N-terminal regions of laminin α, β, and γ domains, collectively known as laminin N-terminal or LN domains. In addition, there is a lower level of sequence identity to bacterial galactose binding domains, which enabled the accurate prediction that LN domains would adopt a similar jelly roll topology[19].

Comparison of netrin G and laminin α5 LN domain sequences (Fig. 3d) reveals an overall correspondence in the alignment that begins subsequent to distinct N-terminal regions. As described above (Fig. 2), in netrin Gs, a ~40aa N-terminal region forms two N-terminal β-strands that extend away from the body of the body of the LN domain to interact with the LE1 domain. By contrast, in the α5 LN domain, the corresponding region spans only ~20aa and lacks the hairpin strand that interacts with LE1 (Fig 3b, d). Although Netrin Gs are more closely related to laminin γ chains, these also lack also the residues forming the hairpin strands found in our structure. Laminin LN domains are characterized by a set of "excursions" from the central jelly roll β-sandwich that is remarkably similar to netrin Gs, with overall similar structures. Although excursion region 1 was largely disordered in the laminin α5 structure (the only currently available structure for an LN domain) its sequence and secondary structure prediction are suggestive of a disulfide-bonded loop structure similar to netrin Gs. The structure of excursion regions 2 and 3 of α5 LN reveal topological similarity to netrin G2 in that each forms a helical subregion, and these regions interact with one another via a small hydrophobic core.

Classical netrin sequences show good alignments with netrin Gs throughout (Fig. 3d), suggesting that they will have a high degree of similarity in their three-dimensional structures. With the exception of one disulfide bond in excursion 1, all four disulfide bonds within the LN domain appear to be conserved between netrins and netrin Gs. The disulfide pattern of their LE domains is identical. In light of the similarity of their overall domain organizations (Fig. 1) it is likely that netrins and netrin Gs adopt very similar three-dimensional structures.

The single known structure of an LN domain-containing protein, that of laminin α5, which also includes two C-terminal LE domains, is superposed on the sNetrin G2 structure in Fig. 3a. The overall RMSD is 3.29Å for 145 corresponding Cα atoms primarily in the LN domain. Overall, the α5 LN domain aligns well with the LN domain found in the sNetrin G2 structure, and the differing orientations of LE domains between α5 LN and sNetrin G2 is apparent by their poor alignment. Superposition of the Netrin G2 LN domain on the LN domain of laminin α5 (Fig. 3b) and superposition of the LE1 domains from LNα5 and sNetrinG2 (Fig. 3c) reveal a high degree of similarity, with RMSDs of 2.95Å for 146 corresponding Cα atoms, and is 0.79Å for 46 corresponding Cα atoms, respectively.

Overall, we observe close similarity between netrin Gs and classical netrins at the sequence level, implying that members of this protein family adopt very similar structures. Despite the

Author Manuscript Author Manuscript Author Manuscript Author Manuscript

overall similarity in comparison to the structure of the N-terminal region of laminin α5, several features unique to the netrin G family are observed. Specifically, a unique β-hairpin structure at the N-terminus and a conserved calcium binding site.

DISCUSSION

The netrin G1 and G2 proteins each bind to a single cognate ligand, NGL-1 and NGL-2, respectively. NGLs contain a 9-repeat N-terminal leucine rich repeat (LRR) region, with similarity to Amigo[22] and Lingo-1[23], and a C-terminal immunoglobulin-like domain linked to a single pass transmembrane segment followed by a cytoplasmic domain that binds the postsynaptic scaffolding protein PSD-95. Prior deletion studies have mapped the site of interaction on NGL1 to the LRR domain, yet the site of interaction on netrin Gs has remained unknown. The ultracentrifugation results we present (Table 1) suggest that the LN domain of netrin Gs includes the NGL interaction region. Briefly, netrin G2 constructs including the LN, all LE domains, or the LN and LE1 domain alone show equivalent interactions with NGL-2. Since we could not produce appropriately folded netrin G2 lacking LE1, we turned to the highly similar netrin G1, for which the LN domain can be produced separately. AUC binding studies of interactions between NGL1 and either netrin G1 LN-LE1 domain (splice isoform f) or the LN domain alone of netrin G1 (splice isoform j) revealed similar interactions, and no requirement for the presence of LE domains. These observations show that, for netrin G1, the LN domain comprises the site of NGL interaction, and by inference netrin G2 is likely to bind NGL-2 in a similar way. In agreement with our data, monoclonal antibodies recognizing the LE1 and C′ domains of netrin G1 and G2, respectively, were not found to block the receptor-ligand interaction[7]. Interestingly, the binding interaction between classical netrins and their cellular receptors, DCC and Unc5h, have also been mapped to the LN domain[24;25]. Given the close sequence similarity between netrins and netrin Gs (Fig. 3), our structure of the ligand binding domain of netrin G2 provides a potential starting point for mutational studies to delineate the DCC/Unc5h binding site of netrins more specifically.

The region of the LN domain responsible for NGL interaction is not known, but structural features of the LN domain limit the possible interaction sites. Two N-linked glycosylation sites (colored magenta in Fig. 4), one of which is conserved in all netrin Gs, create protrusions that likely exclude these surfaces from mediating specific molecular interactions. Additionally, the Ca^{2+} binding site, on the opposite molecular face from these glycans, is also unlikely to be involved in binding due to the Ca^{2+} independence of netrin G/NGL interactions evidenced by our AUC studies and prior cell binding assays[4]. Netrin G1 and G2 show mutually exclusive affinity for their respective ligands, NGL-1 and NGL-2[4; 5; 7; 8]. To identify possible sites of specificity, we therefore mapped the positions of residues conserved among netrins G1s and conserved among netrin G2s, but which differ between the two subfamilies, to the molecular surface of the LN domain of netrin G2 (colored in green in Fig. 4). These potential specificity sites map widely over the LN domain. This pattern could be obtained due to the large binding surface expected for interactions between LRR regions which typically bind large surfaces and can envelop binding partners through their concave face (Fig. 4,[26; 27]). NGL LRR regions include 9 LRR repeats, too few to form a near-closed circle, and more likely to represent a crescent-shaped molecule. We note that

Author Manuscript Author Manuscript Author Manuscript Author Manuscript

the most likely netrin G NGL binding surface – formed by the excursions of the β-jelly roll domain– has a convex shape that appears to closely complement the concave surface expected for the NGL LRR region (Fig. 4). Future mutagenesis and/or structural studies will be needed to define this interaction in detail.

Both netrins G1 and G2 are subject to alternative splicing. Netrin G1 can be produced in up to 14 alternative splice forms[1; 6; 11], and three netrin G2 alternatively spliced isoforms have been reported[1; 6]. These alternative splice forms correspond to either deletions of LE domains, or small insertions within the LE domain region. Since, as we have shown above, binding between netrin Gs and NGLs depends only on the netrin G LN domain region, it is unlikely that alternative splicing will directly affect netrin G/NGL interaction. Thus, it seems likely that alternative splicing of netrin Gs will serve a role other than to modulate their interaction with NGLs. We speculate that alternative splicing might regulate interactions with other yet unknown binding partners in *cis*, which appear to be necessary for induction of presynaptic differentiation following ligation by NGLs[4].

The AUC measurements we performed reveal binding affinities of ~ 505 nM and ~191 nM for interactions of netrins G1 and G2 with their respective cognate NGLs. These K_D values are comparable to those previously determined by SPR[5], but are weaker by 5–10 fold from results of solid-phase binding assays that employed NGL proteins fused to antibody Fc regions and were thus constitutively dimeric[3; 8]. This would be expected to increase the apparent affinity due to avidity effects and thus underestimate K_D. The correspondence between our K_D determinations and those made previously for monomeric proteins suggests that these represent the true solution binding affinities.

Our results strongly suggest that the recognition complex between netrin Gs and NGLs is formed by interactions between the LN domain of netrin Gs and the LRR region of NGLs. Our AUC results show that both netrin Gs and NGLs are monomers in solution, and form complexes with 1:1 stoichiometry. Thus, while the data reported here reveal the overall outlines of netrin G/NGL recognition, the mechanism by which binding induces signal transduction cannot be inferred from our results, and must await further study.

MATERIALS AND METHODS

Mammalian protein production

Coding sequences for human netrin G2, spanning the full ectodomain (LN domains, LE1-3 and C′; Asp1-Arg487 of the mature ‘a’ isoform), and “short” sNetrin G2, spanning only LN and LE1 domains (Asp1- Ser332 of the mature protein), preceded by their native signal sequence with a Kozak sequence and excluding the GPI-anchor attachment site, were amplified by PCR from cDNA image clone 4344617, with an octa histidine tag at their C-terminus. Products were cloned into the episomal expression vector pCEP4 (Invitrogen) using restriction sites HindIII/NotI. Coding sequences for mouse netrin G1 isoforms G1f and G1j (His1-Lys336 and His1-Arg268 of the mature proteins, respectively) were amplified by PCR from cDNA image clone 6837530 preceded by their native signal sequence and followed by a C-terminal hexa histidine tag and were subsequently cloned into pCEP4 using the restriction sites KpnI/NotI. For the extracellular fragments of human NGL-2 and mouse

Author Manuscript Author Manuscript Author Manuscript Author Manuscript

NGL-1, coding sequences spanning the LRR and Ig domains (Gln1- Thr414 and Gln1-Ser417 of the mature protein, respectively), preceded by a Kozak sequence and their native signal sequence, with their C-terminal stalk region, transmembrane and cytoplasmic domains replaced by a hexa histidine tag, were amplified from cDNA image clones 40068146 and 30617370, and cloned into pCEP4 using the restriction sites HindIII/NotI and KpnI/NotI, respectively.

For protein expression, human embryonal kidney (HEK) 293 GNTI$^-$ cells were transfected in 6 well plates using Lipofectamine 2000 (Invitrogen) according to the manufacturer's manual. During continuous selection with 200_g/ml Hygromycin B for stable expression, proteins were secreted into growth medium comprising DMEM/F12 supplemented with 10% newborn calf serum, 100 units/ml Penicillin, 100μg/ml Streptomycin and 4mM L-Glutamine and were then purified from 4 liters of conditioned media. After supplementing the conditioned media with 500mM sodium chloride, 20mM Tris-Cl pH8.0, 3mM calcium chloride and 20mM imidazole pH8.0, His-tagged proteins were extracted from the medium by batch affinity purification by adding 20mL of nickel charged IMAC resin (GE), pre-equilibrated in binding buffer (500mM sodium chloride, 20mM Tris-Cl pH8.0, 3mM calcium chloride and 20mM imidazole pH8.0). After 3 hours of incubation the resin was collected from supernatant by passing through Kontes columns and was washed with 20 column volumes of binding buffer followed by 20 column volumes of the same buffer with increased imidazole concentration (25mM). Proteins were eluted with five column volumes of the same buffer containing 90mM Imidazole for netrin G2 and NGL2 preparations or 75mM imidazole for netrin G1 and NGL-1. Eluted proteins were dialyzed over night at 4°C into a low ionic strength buffer of 100mM sodium chloride, 10mM Bis-Tris pH6.0 and 3mM $CaCl_2$. Further purification by flowing through a Mono S HR 10/10 ion exchange column (GE) and size exclusion chromatography with HiLoad 26/60 Superdex^{TM} S200 prepgrade (GE) yielded pure proteins in a buffer of 150mM NaCl, 10mM Tris-Cl pH8.0, 3mM $CaCl_2$ at protein concentrations of 1 to 10mg/mL. In addition, NGL-1 and NGL-2 were treated with Endoglycosidase H (New England Biolabs) after the ion exchange step and then separated from glycosylated protein by flowing through Mono Q HR 10/10 (GE) prior to size exclusion. Proteins were flash frozen and stored at −80°C.

Analytical ultracentrifugation

We performed equilibrium analytical ultracentrifugation (AUC) experiments using a Beckman XLA/I ultracentrifuge, with a Ti50An or Ti60An rotor. Prior to each experiment, all proteins were diluted with buffer (150mM NaCl, 10mM Bis-Tris pH6.0, 3mM $CaCl_2$ or 1mM EDTA pH8.0, 10% glycerol) and dialyzed for 16 hours at 4°C in the same buffer. 120_L of proteins at three different concentrations 0.7mg/mL, 0.46mg/mL and 0.24mg/mL were loaded into six-channel equilibrium cells with parallel sides and sapphire windows. We performed all experiments at 25°C and collected data using either both UV at 280nm and interference at 660nm, or UV alone. All proteins were spun for 20 hours at 12,300*g* and four scans (1 per hour) were collected, speed was increased to 18,600*g* for 10 hours and four scans (1 per hour) were collected and speed was increased to 26,200*g* for another 10 hours and four scans (1 per hour) were taken. Finally, speed was increased to 35,200*g* to yield 96 or 48 scans in total per sample. Relative centrifugal forces are given at the measuring cell

Author Manuscript Author Manuscript Author Manuscript Author Manuscript

center at a radius of 65mm. Buffer density and protein v-bars were calculated using the program SednTerp (Alliance Protein Laboratories), and we analyzed the collected data using HeteroAnalysis 1.1.44 (http://www.biotech.uconn.edu/auf). We fitted data from all concentrations and speeds globally by nonlinear regression to either a monomer-dimer equilibrium model or an ideal monomer model. All experiments were performed at least in duplicate. Presence of 10% glycerol in the running buffer improved protein stability and solubility. We also confirmed that the measured K_D for Netrin G2 and NGL-2 was identical in the absence of glycerol. Covalent molecular weights were determined by mass spectrometry for netrin G2, sNetrin G2 and NGL-2 and Netrin G1j, G1f and NGL-1 are listed in table 1.

Crystallization and structure determination

We expressed and purified human sNetrin G2 as described above and used it for crystallization studies at a concentration of 10.3 mg/mL. Using the vapor diffusion method, protein crystals grew at 20°C within 48h after combining 2_L protein with 1_L well solution composed of 20% (w/v) PEG 3,350, 200mM calcium acetate and 100mM sodium cacodylate pH6.5. Crystals were flash frozen in liquid nitrogen after being briefly immersed in cryo protectant (30% (w/v) sucrose, 18% (w/v) PEG 3,350, 200mM calcium acetate, 100mM sodium cacodylate pH6.5).

Native data was collected on a single frozen crystal at the X4A beamline of the National Synchrotron Light Source, Brookhaven National Laboratory at a wavelength of 1.071Å. We processed the data using the HKL suite [28].

Phases were obtained using a sulfur single wavelength anomalous diffraction (SAD) experiment at Fe K_ edge (E=7.112 keV). Data was collected for five separate native sNetrin G2 crystals under cryostream protection at 100K. For each crystal, we used the inverse beam data collection mode and collected 360 x 2 frames with an oscillation angle of 1 degree. The data was collected at a detector-to-sample distance at 120mm and a helium-gas-purging cone was inserted between crystal and detector to reduce air absorption at 7.112 keV. Crystals were mounted on MiTiGen dual thickness polyimide mounts with suitable sizes to further reduce absorption during data collection. All sulfur anomalous diffraction data sets were measured by an ADSC Quantum 4R detector and we processed the data using XDS [29] and CCP4 [30] packages. Data collection and reduction statistics for the best experiment are listed in Table 2.

The sulfur substructure was determined by SHELX/C-D [31] either from the 5-crystal data or from the best single-crystal data. The protein contains 10 disulfides and 9 methionine residues, of which the disulfides were treated as 10 super atoms. Therefore a total of 19 sites were used for substructure determination. From 100 SHELXD tries, 21 solutions were found with highest CCall/CCweak of 43.78/21.91. The substructure was then refined and SAD phases were calculated using Phaser [32] for a data range between 30 and 2.3 Å (Table 2). The figure of merit from Phaser is 0.343 and increased to 0.796 after density modification by DM [30] with an estimated solvent content of 58%. The electron density was of high quality and allowed automatic model building by ARP/wARP [15] at 2.3 Å. The obtained model was

Author Manuscript Author Manuscript Author Manuscript Author Manuscript

further refined against the 1.8 Å high resolution native data and a subsequent ARP/wARP run was started for model re-building.

Further refinement was carried out by cycles of manual building in Coot [16] followed by automated refinement in Refmac [17; 30]. The refined model contains 331 amino acids, two N-linked sugars, one calcium ion, two phosphate ions and 588 water molecules. Ramachandran plot statistics for the final model were calculated using molprobity [33] and are 95.4% favored, 100% allowed and 0% disallowed; data collection and refinement statistics for native and S-SAD data are summarized in Table 2.

Acknowledgments

We thank Prof. T. M. Jessell for helpful discussions and suggestions on the manuscript. X-ray data were acquired at the X4A and X4C beamlines of the National Synchrotron Light Source, Brookhaven National Laboratory, a DOE facility; the beamlines are supported by the New York Structural Biology Center. We thank John Schwanof and Randy Abramowitz for help with synchrotron data collection. This work was supported by NIH grant GM62270 to LS.

Abbreviations

NGL	Netrin G Ligand
S-SAD	sulfur single wavelength anomalous diffraction
LE domain	laminin- epidermal growth factor like domain
LN domain	laminin N-terminal domain
GPI	glycosyl-phosphatidyl-inositol
LRR	leucine rich repeat
AUC	analytical ultra centrifugation
HEK 293 cells	human embryonal kidney 293 cells
GNTI	N-acetyl-glucosaminyl transferase I
SPR	Surface Plasmon Resonance
Ig	immunoglobulin

References

1. Nakashiba T, Nishimura S, Ikeda T, Itohara S. Complementary expression and neurite outgrowth activity of netrin-G subfamily members. Mech Dev. 2002; 111:47–60. [PubMed: 11804778]
2. Nakashiba T, Ikeda T, Nishimura S, Tashiro K, Honjo T, Culotti JG, Itohara S. Netrin-G1: a novel glycosyl phosphatidylinositol-linked mammalian netrin that is functionally divergent from classical netrins. J Neurosci. 2000; 20:6540–50. [PubMed: 10964959]
3. Lin JC, Ho WH, Gurney A, Rosenthal A. The netrin-G1 ligand NGL-1 promotes the outgrowth of thalamocortical axons. Nat Neurosci. 2003; 6:1270–6. [PubMed: 14595443]
4. Kim S, Burette A, Chung HS, Kwon SK, Woo J, Lee HW, Kim K, Kim H, Weinberg RJ, Kim E. NGL family PSD-95-interacting adhesion molecules regulate excitatory synapse formation. Nat Neurosci. 2006; 9:1294–301. [PubMed: 16980967]

Author Manuscript Author Manuscript Author Manuscript Author Manuscript

5. Nishimura-Akiyoshi S, Niimi K, Nakashiba T, Itohara S. Axonal netrin-Gs transneuronally determine lamina-specific subdendritic segments. Proc Natl Acad Sci U S A. 2007; 104:14801–6. [PubMed: 17785411]
6. Yin Y, Miner JH, Sanes JR. Laminets: laminin- and netrin-related genes expressed in distinct neuronal subsets. Mol Cell Neurosci. 2002; 19:344–58. [PubMed: 11906208]
7. Niimi K, Nishimura-Akiyoshi S, Nakashiba T, Itohara S. Monoclonal antibodies discriminating netrin-G1 and netrin-G2 neuronal pathways. J Neuroimmunol. 2007; 192:99–104. [PubMed: 17945353]
8. Zhang W, Rajan I, Savelieva KV, Wang CY, Vogel P, Kelly M, Xu N, Hasson B, Jarman W, Lanthorn TH. Netrin-G2 and netrin-G2 ligand are both required for normal auditory responsiveness. Genes Brain Behav. 2008; 7:385–92. [PubMed: 17973922]
9. Barallobre MJ, Pascual M, Del Rio JA, Soriano E. The Netrin family of guidance factors: emphasis on Netrin-1 signalling. Brain Res Brain Res Rev. 2005; 49:22–47. [PubMed: 15960985]
10. Colognato H, Yurchenco PD. Form and function: the laminin family of heterotrimers. Dev Dyn. 2000; 218:213–34. [PubMed: 10842354]
11. Meerabux JM, Ohba H, Fukasawa M, Suto Y, Aoki-Suzuki M, Nakashiba T, Nishimura S, Itohara S, Yoshikawa T. Human netrin-G1 isoforms show evidence of differential expression. Genomics. 2005; 86:112–6. [PubMed: 15901489]
12. Woo J, Kwon SK, Kim E. The NGL family of leucine-rich repeat-containing synaptic adhesion molecules. Mol Cell Neurosci. 2009; 42:1–10. [PubMed: 19467332]
13. Ko J, Kim E. Leucine-rich repeat proteins of synapses. J Neurosci Res. 2007; 85:2824–32. [PubMed: 17471552]
14. Liu Q, Zhang Z, Dahmane T, Assur Z, Brasch J, Marcia F, Shapiro L, Hendrickson WA. Structures from anomalous diffraction of native biological macromolecules. 2011 to be submitted.
15. Langer G, Cohen SX, Lamzin VS, Perrakis A. Automated macromolecular model building for X-ray crystallography using ARP/wARP version 7. Nat Protoc. 2008; 3:1171–9. [PubMed: 18600222]
16. Emsley P, Cowtan K. Coot: model-building tools for molecular graphics. Acta Crystallographica Section D-Biological Crystallography. 2004; 60:2126–2132.
17. Murshudov GN, Vagin AA, Dodson EJ. Refinement of macromolecular structures by the maximum-likelihood method. Acta Crystallogr D Biol Crystallogr. 1997; 53:240–55. [PubMed: 15299926]
18. Hussain SA, Carafoli F, Hohenester E. Determinants of laminin polymerization revealed by the structure of the alpha5 chain amino-terminal region. EMBO Rep. 2011; 12:276–82. [PubMed: 21311558]
19. Kalkhof S, Haehn S, Paulsson M, Smyth N, Meiler J, Sinz A. Computational modeling of laminin N-terminal domains using sparse distance constraints from disulfide bonds and chemical cross-linking. Proteins-Structure Function and Genetics. 2010; 78:3409–27.
20. Boraston AB, Ficko-Blean E, Healey M. Carbohydrate recognition by a large sialidase toxin from Clostridium perfringens. Biochemistry. 2007; 46:11352–60. [PubMed: 17850114]
21. Stetefeld J, Mayer U, Timpl R, Huber R. Crystal structure of three consecutive laminin-type epidermal growth factor-like (LE) modules of laminin gamma1 chain harboring the nidogen binding site. Journal of Molecular Biology. 1996; 257:644–57. [PubMed: 8648630]
22. Chen Y, Aulia S, Li L, Tang BL. AMIGO and friends: an emerging family of brain-enriched, neuronal growth modulating, type I transmembrane proteins with leucine-rich repeats (LRR) and cell adhesion molecule motifs. Brain Res Rev. 2006; 51:265–74. [PubMed: 16414120]
23. Mosyak L, Wood A, Dwyer B, Buddha M, Johnson M, Aulabaugh A, Zhong X, Presman E, Benard S, Kelleher K, Wilhelm J, Stahl ML, Kriz R, Gao Y, Cao Z, Ling HP, Pangalos MN, Walsh FS, Somers WS. The structure of the Lingo-1 ectodomain, a module implicated in central nervous system repair inhibition. Journal of Biological Chemistry. 2006; 281:36378–90. [PubMed: 17005555]
24. Qin S, Yu L, Gao Y, Zhou R, Zhang C. Characterization of the receptors for axon guidance factor netrin-4 and identification of the binding domains. Mol Cell Neurosci. 2007; 34:243–50. [PubMed: 17174565]

Author Manuscript Author Manuscript Author Manuscript Author Manuscript

25. Rajasekharan S, Kennedy TE. The netrin protein family. Genome Biol. 2009; 10:239. [PubMed: 19785719]
26. Schubert WD, Urbanke C, Ziehm T, Beier V, Machner MP, Domann E, Wehland J, Chakraborty T, Heinz DW. Structure of internalin, a major invasion protein of Listeria monocytogenes, in complex with its human receptor E-cadherin. Cell. 2002; 111:825–36. [PubMed: 12526809]
27. Morlot C, Thielens NM, Ravelli RB, Hemrika W, Romijn RA, Gros P, Cusack S, McCarthy AA. Structural insights into the Slit-Robo complex. Proc Natl Acad Sci U S A. 2007; 104:14923–8. [PubMed: 17848514]
28. Otwinowski Z, Minor W. Processing of X-ray diffraction data collected in oscillation mode. Macromolecular Crystallography, Pt A. 1997; 276:307–326.
29. Kabsch W. Xds. Acta Crystallogr D Biol Crystallogr. 2010; 66:125–32. [PubMed: 20124692]
30. Bailey S. The Ccp4 Suite - Programs for Protein Crystallography. Acta Crystallographica Section D-Biological Crystallography. 1994; 50:760–763.
31. Sheldrick GM. A short history of SHELX. Acta Crystallogr A. 2008; 64:112–22. [PubMed: 18156677]
32. McCoy AJ, Grosse-Kunstleve RW, Adams PD, Winn MD, Storoni LC, Read RJ. Phaser crystallographic software. Journal of Applied Crystallography. 2007; 40:658–674. [PubMed: 19461840]
33. Chen VB, Arendall WB 3rd, Headd JJ, Keedy DA, Immormino RM, Kapral GJ, Murray LW, Richardson JS, Richardson DC. MolProbity: all-atom structure validation for macromolecular crystallography. Acta Crystallogr D Biol Crystallogr. 2010; 66:12–21. [PubMed: 20057044]
34. Kabsch W, Sander C. Dictionary of protein secondary structure: pattern recognition of hydrogen-bonded and geometrical features. Biopolymers. 1983; 22:2577–637. [PubMed: 6667333]

Author Manuscript Author Manuscript Author Manuscript Author Manuscript

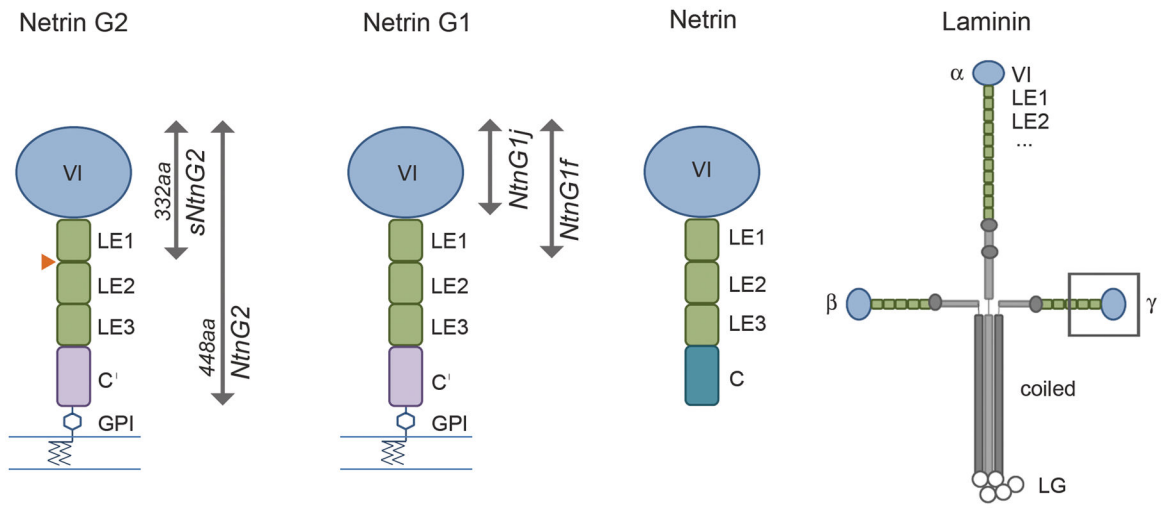

Fig. 1. Schematic representation of domain structures of netrin Gs, classical netrins and laminin

Netrin Gs share a domain structure similar to classical netrins and the N-terminal region of laminin α, β, and γ chains: each is characterized by a large N-terminal domain, the LN domain (blue), followed by three or more LE domains. Classical netrins, at their C-terminus, include a region (domain C) which is characterized by basic residues and interacts with extracellular matrix components. Netrin Gs have an analogous region, the C′ domain, which has hydrophobic character and includes an attachment site for a GPI membrane anchor. By contrast, laminins contain additional LE domains, followed by oligomerization regions that mediate formation of the classic laminin cross structure. Netrin Gs are alternatively spliced in their LE domain regions. The orange triangle indicates the site of alternative exons for netrin G2, which add either 59 (isoform B) or 34 (isoform C) amino acid residues. Alternative splicing for netrin G1 encodes 14 distinct isoforms, some of which correspond to soluble proteins such as the J and F isoforms indicated in the figure.

Author Manuscript
Author Manuscript
Author Manuscript
Author Manuscript

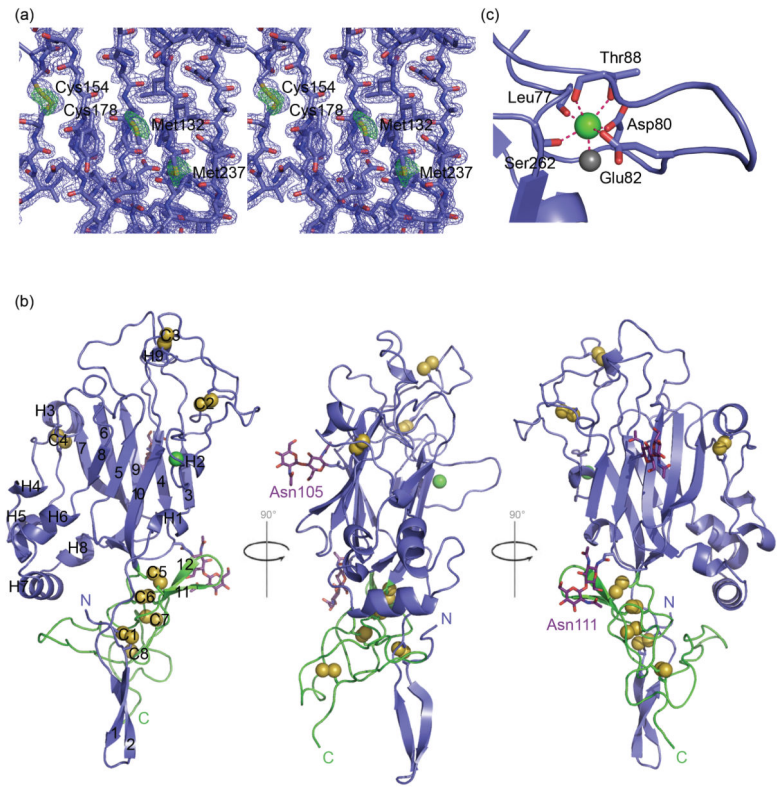

Fig. 2. Structure of sNetrin G2

(a) Stereo representation of the experimental electron density at 1.8Å resolution produced by Sulfur-SAD phasing, contoured at 1.0σ. The Bijvoet difference Fourier map, contoured at 3.5σ, is shown in green. (b) Ribbon representation of the structure of sNetrin G2, comprised of the LN (blue) and LE1 domain (green). Secondary structure elements are labeled, disulfide bonds are shown with space filling models of the bonded γ-sulfur atoms. The glycans from two glycosylation sites, Asn 105 and Asn 111, are drawn in stick representation, and the single bound Ca^{2+} ion is shown as a green sphere. (c) Expanded view of Ca^{2+} binding site. The Ca^{2+} ion is coordinated by backbone carbonyl groups from Leu77, Thr88, and Ser262, and side chains from Asp80, Leu82, and Thr88. An additional ligand is provided by a bound water molecule shown as a gray sphere.

Author Manuscript Author Manuscript Author Manuscript Author Manuscript

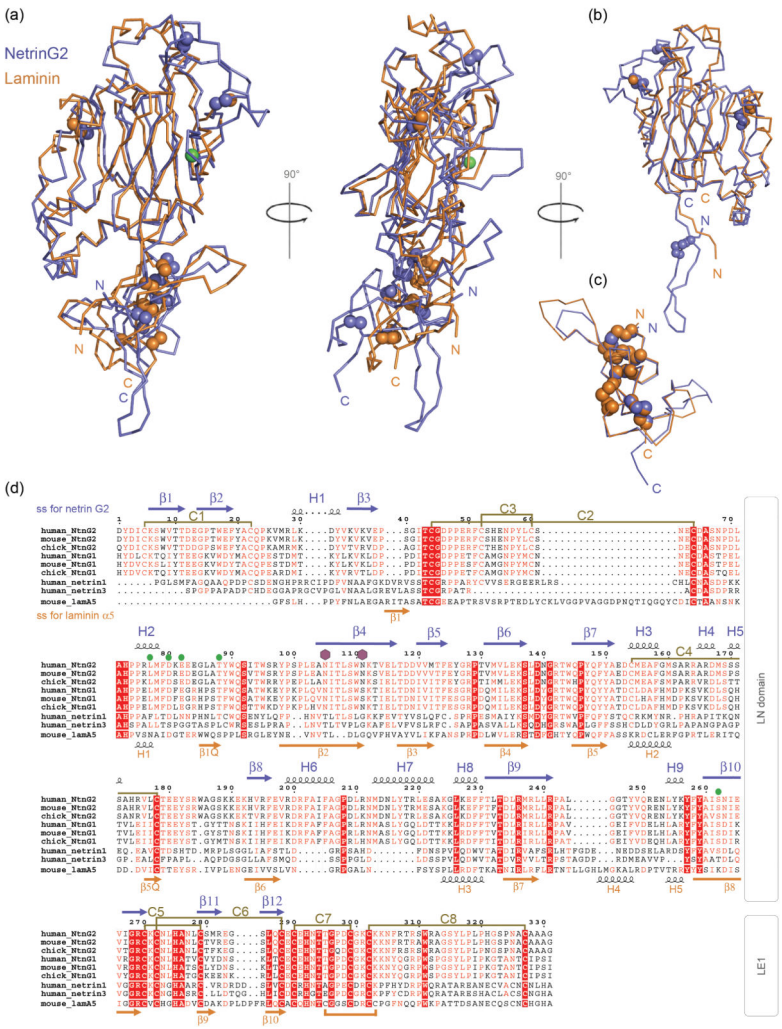

Fig. 3. Comparison of sNetrin G2 with related proteins

(a) Superposed Cα traces of sNetrin G2 (blue) and the corresponding region from laminin α5 (orange; PDB 2Y38) shown in two orthogonal views. (b) Superposition of the LN domain regions alone. (c) Superposition of the LE1 domains. (d) Multiple sequence alignment of the LN and LE1 domain regions of netrin Gs 1 and 2 from human, mouse, and chicken, as well as human netrins 1 and 3 and mouse laminin α5. Secondary structure, assigned by DSSP[34], is shown in blue above the alignment for sNetrin G2 and below in orange for laminin α5. All sNetrin G2 helices are in the α conformation, with the exception of short helices H1, H2, H4, and H5, which adopt the 3_{10} conformation. Disulfide bonds in sNetrin G2 are drawn in gold between paired cysteines. Laminin α5 contains one disulfide bond not found in sNetrin G2, drawn in gold below the alignment. Green filled circles indicate residues involved in calcium coordination, purple hexagons indicate N-linked glycosylation.

Author Manuscript Author Manuscript Author Manuscript Author Manuscript

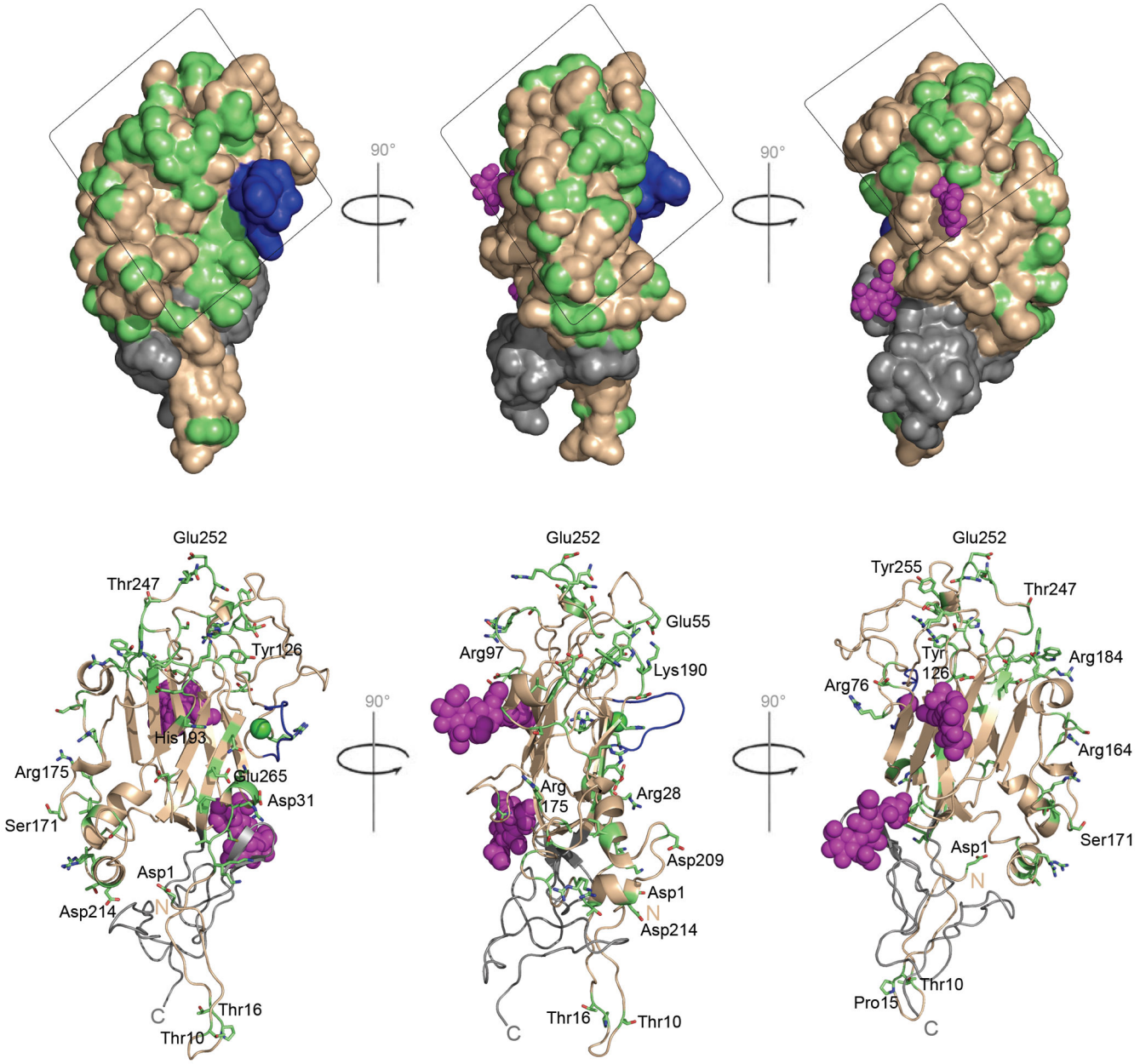

Fig. 4. Surface representation of sequence conservation between netrin Gs 1 and 2

Netrin Gs 1 and 2 bind to NGL1 and NGL2, respectively, but show no cross-interaction. Upper panel: Differences between the surfaces of netrin Gs 1 and 2 are likely to underlie this specificity. The figure shows three orthogonal views of sequence conservation mapped to the netrin G2 LN domain structure. The boxed region highlights the largest continuous areas of residues that differ in character between netrins G 1 and 2, indicating a possible NGL binding region. The LE1 domain, which does not partake in NGL binding, is shown in gray. The Ca2+ binding region is blue, and glycans are shown in magenta. Residues of conserved character between human netrin G1 and G2 are shown in a wheat color, and non-conservative substitutions are shown in green. Residues deemed to have conserved character

Author Manuscript Author Manuscript Author Manuscript Author Manuscript

included the following 5 groups: VILMA; YFW; RKH; STQN; ED. Lower Panel: Ribbon representations of sNetrin G2 are shown in the lower panel in same orientation and color coding as upper panel. Residues of nonconservative residues are represented as sticks.

Author Manuscript

Author Manuscript

Author Manuscript

Author Manuscript

Table 1

Equilibrium AUC analysis of Netrin G and NGL binding

Protein	Oligomeric state	Apparent Mw (Da)	K_D dimerization (nM)	Determined MW (Da)
Netrin G2	Monomer	60 417	-	62 496[2]
sNetrin G2	Monomer	38 303	-	42 153
NGL 2	Monomer	46 697	-	50 517
Netrin G2 + NGL 2	Dimer	100 112	190.5 ± 28.5[1]	113 013[3]
Netrin G2 + NGL 2 (EDTA)	Dimer	98 072	264.5 ± 0.5	113 013
sNetrin G2 + NGL 2	Dimer	87 474	180 ± 14	92 670
Netrin G1f	Monomer	44 554	-	40 748
Netrin G1j	Monomer	31 229	-	33 525
NGL 1	Monomer	57 151	-	60 860
Netrin G1f + NGL 1	Dimer	88 199	505 ± 245	101 608
Netrin G1j + NGL 1	Dimer	74 095	1 490 ± 150	94 385

[1] Errors given represent standard deviation for two separate experiments.

[2] Molecular weights listed were determined by mass spectrometry.

[3] Molecular weights for complexes calculated by addition of MWs of components found in the complex (A(MW) + B (MW) = AB (MW))

Author Manuscript Author Manuscript Author Manuscript Author Manuscript

Table 2

Crystallographic data and refinement statistics.

	sNetrin G2 (native)	sNetrin G2 (sulfur)
Data collection		
Space group	$P3_22\ 1$	$P3_22\ 1$
Cell dimensions a=b, c (Å); α, β, γ (°)	64.13, 190.64; 90, 90, 120	63.33, 191.27; 90, 90, 120
Resolution (Å)	30-1.8 (1.86-1.80)	30-2.3 (2.36-2.3)
R_{merge} (%)	6.9 (27.4)	5.3 (3.5)
I/σI	19. 6 (4.2)	53.9 (3.5)
Completeness	95.4 (74.8)	96.6 (72.2)
Redundancy	5.6 (4.6)	32.7 (9.9)
Observed reflections	228,776	652,303
Unique reflections	40,558	19,948
SHELXD[1] CCall/CCweak		43.8/21.9
FOM		0.343
FOM after DM		0.796
Refinement		
Resolution (Å)	15-1.8	
Number of reflections	38,026	
R_{work}	18.2	
R_{free}	23.1	
Number of atoms	2,782	
Protein	3,247	
Carbohydrate	56	
Calcium Ion	1	
Chloride Ion	2	
Phosphate	2	
Water	588	
R. m. s. deviations		
Bond length (Å)	0.027	
Bond angles (°)	2.6	
Mean B factors (Å^2)		
Protein	27.3	
Carbohydrate	49.2	
Ion	41.4	
Phosphate	38.6	
Water	39.5	
Ramachandran plot		
Outliers (%)	0	
Favored (%)	95.4	
Allowed (%)	4.6	

[1] SHELXD was used for substructure determinuation with data between 30 and 3.0Å.

Values in parentheses are from the highest resolution shell.

Author Manuscript
Author Manuscript
Author Manuscript
Author Manuscript